INTERNATIONAL JOURNAL OF CLIMATOLOGY
Int. J. Climatol. (2018)
Published online in Wiley Online Library
(wileyonlinelibrary.com) DOI: 10.1002/joc.5419

RMetS Royal Meteorological Society

Short Communication

Activity of the Southern Annular Mode during 2015–2016 El Niño event and its impact on Southern Hemisphere climate anomalies

Carolina S. Vera[a,b]* and Marisol Osman[a,b]

[a] *Departamento de Ciencias de la Atmósfera y los Océanos, Facultad de Ciencias Exactas y Naturales, Buenos Aires, Argentina*
[b] *Centro de Investigaciones del Mar y la Atmósfera (CIMA), Instituto Franco-Argentino del Clima y sus Impactos (UMI-IFAECI)/CNRS, CONICET, Universidad de Buenos Aires, Buenos Aires, Argentina*

ABSTRACT: Previous studies documented that El Niño (EN) events are in general associated with negative phases of the Southern Annular Mode (SAM). EN 2015–2016 (EN15–16) was one of the three strongest events ever recorded. However, it was associated with a SAM positive phase of extreme intensity. Furthermore, while the negative linear relationship between ENSO and SAM during the most recent period (1986–2014) was significant and associated with a narrow uncertainty band, the combined condition of both climate patterns in the EN15–16 event was an outlier. The EN15–16 influence on the austral summer circulation anomalies at the extratropical and polar regions of the Southern Hemisphere was considerably altered by the strong SAM positive phase, which was evident not only at the troposphere but also at the stratosphere. Such circulation changes resulted in unusual regional impacts, such as negative anomalies of surface air temperature in western Antarctic Peninsula and negative precipitation anomalies in southeastern South America, ever recorded for previous strong EN events. Further research is needed to better understand the mechanisms explaining the SAM behaviour during 2015–2016 and its implication for climate predictability on seasonal timescales.

KEY WORDS SAM; PSA patterns; ENSO; southeastern South America

Received 19 June 2017; Revised 20 December 2017; Accepted 22 December 2017

1. Introduction

The Southern Annular Mode (SAM) is the leading pattern of circulation anomaly variability in the Southern Hemisphere (SH). Its spatial characteristics and temporal evolution are usually described by the first leading pattern resulted from an empirical orthogonal function analysis of the geopotential-height anomalies (e.g. Kidson, 1988). SAM spatial distribution is characterized by a centre of circulation anomalies extended over Antarctica and anomalies of opposite sign at middle latitudes, generally associated with a 3–4 wavenumber structure. SAM activity is fundamentally maintained by the atmosphere internal variability through mean flow-perturbation interaction, exhibiting variability on a wide range of timescales from subseasonal to interannual and longer timescales (e.g. Kidson, 1999). Also, the pattern exhibits a significant linear trend towards more frequent positive phases, which are associated with negative geopotential-height anomalies over polar regions (e.g. Marshall, 2003). SAM trend is present in all seasons, although it is larger in DJF (e.g. Arblaster and Meehl, 2006). The trend has been identified as driven by the combined effect of the increasing greenhouse gases and the stratospheric ozone depletion, being the latter recognized by many previous publications as the dominant forcing mechanism, especially in the upper troposphere and the stratosphere (e.g. Arblaster and Meehl, 2006; Arblaster *et al.,* 2011).

SAM and ENSO activity can be significantly correlated, with a preference for the occurrence of SAM negative phases during EN events and SAM positive phases during La Niña (LN) events (e.g. Clem and Fogt, 2013, and the references therein). In both cases, transient momentum fluxes increase in the South Pacific, reinforcing ENSO teleconnections (Fogt *et al.,* 2011). In turn, the circulation anomalies strengthened by such combined influence modulate climate variability in the Antarctic Peninsula (e.g. Clem and Fogt, 2013) and southern South America (e.g. Vera and Silvestri, 2009). Moreover, SAM negative (positive) phases can reinforce (weaken) the circulation anomalies induced by EN events in the South Pacific Ocean (e.g. Vera *et al.,* 2004). However,

* Correspondence to: C. S. Vera, Centro de Investigaciones del Mar y la Atmósfera, Facultad de Ciencias Exactas y Naturales, Universidad de Buenos Aires, Ciudad Universitaria, Pabellón 2, Piso 2, Zip: 1432, Buenos Aires, Argentina. E-mail: carolina@cima.fcen.uba.ar

the SAM–ENSO relationship exhibits multidecadal variations (e.g. Fogt and Bromwich, 2006). Silvestri and Vera (2009) show that during the austral spring, the correlation between SAM and ENSO was negligible between 1960s and 1970s while it was significant and negative in the 1980s–1990s.

The climate monitoring performed throughout the EN event that developed between 2015 and 2016 (hereafter referred as EN15–16) shows that although it was one of the most intense events ever registered, it was in general associated with a strong SAM positive phase. The analysis of the 2015 climate conditions in the SH made by Fogt (2016) explains at least in part the SAM behaviour. During austral winter 2015, the dynamics associated with the wave activity in the SH was weaker than normal and promoted a very stable and cold polar vortex. The latter in turn promoted larger-than-usual polar ozone losses and a near-record ozone hole that was among the largest in area coverage and most persistent. The state of climate 2015 report concluded that the persistently colder-than-normal temperatures enabled larger ozone depletion by human-produced chlorine and bromine compounds, which are still at fairly high levels. Moreover, between October and the end of December 2015, the polar vortex remained quite strong in response to the persistent stratospheric cooling with positive zonal winds exceeding 1–2 standard deviations above the normal values, thus explaining the strong SAM positive phase. The 2015 ozone hole broke up by the end of December, 2 weeks later than average. The reasons explaining why the tropospheric westerlies remained stronger than normal during January and February 2016 have not been analysed by the scientific community yet. However, there are some mechanisms that can explain such behaviour. Baldwin and Dunkerton (2001) show that large variations in the strength of the stratospheric circulation can descend from the upper to lower stratosphere and in turn influence tropospheric circulation during the 60 days after the onset of stratospheric circulation anomalies.

The conditions that characterized the southern polar regions between 2015 and 2016 altered the response of the extratropical circulation in the SH typically expected in strong EN events such as the EN15–16. In particular, Fogt (2016) shows that between September and December 2015, the EN-induced teleconnections in the South Pacific were displaced northward, altering in turn the EN impact over the Antarctica. Therefore, the purpose of this work is to analyse the main characteristics of the SAM activity between 2015 and 2016, and its role in modulating the EN15–16 influence on climate anomalies in the SH. Special focus is made in describing the associated impact on climate anomalies over the Antarctic Peninsula and southeastern South America (SESA). The paper is organized as follows: section 2 describes the data and methodology, section 3 assesses the ENSO-SAM relationship, including an analysis of the related climate anomalies in the SH and the associated impacts over both, Antarctic Peninsula, and SESA, and conclusions are presented in section 4.

2. Data and methodology

Monthly means of geopotential heights and surface air temperature from the National Centers for Environmental Prediction–National Center for Atmospheric Research (NCEP–NCAR) reanalysis dataset (Kalnay *et al.,* 1996) were used on a 2.5° latitude × 2.5° longitude grid. The period considered for the historical analysis goes from April 1957 to March 2015. Given that the quality of the NCEP Reanalysis in the SH before 1979 is questionable, due to the sparse upper air observation network available and the lack of satellite data, its impact on the results have been lessened by defining anomalies as departures from the corresponding long-term climatological seasonal means and then linearly detrended. In addition, as it is described later, the study is based on overall composites that include a small portion of data before 1979, and that they are consistent with previous publications addressing ENSO influence on the circulation anomalies in the SH (e.g. Mo, 2000; Vera *et al.,* 2004). Hereafter, seasons are referred as those for the SH.

The SAM index defined by Marshall (2003) (available at http://www.nerc-bas.ac.uk/icd/gjma/sam.html) was considered. It is based on the differences between normalized monthly zonal means of sea-level-pressure observations at 40 and 65°S. A seasonal SAM index was computed performing 3-month running averages to the corresponding monthly values.

The historical EN events (Hist_EN) considered in the study are the following: 1951, 1953, 1957, 1963, 1965, 1968, 1969, 1972, 1976, 1977, 1982, 1986, 1987, 1991, 1994, 1997, 2002, 2004, 2006, and 2009. They were selected from those identified by the Climate Prediction Center (CPC) based on a threshold of ±0.5 °C for the Oceanic Niño Index (ONI). The ONI is defined as the 3-month running mean of sea-surface temperature (SST) anomalies from the ERSST.v4 dataset in the Niño 3.4 region (5°N–5°S, 120°–170°W). The information of historical ONI values and the associated ENSO events are available at www.cpc.ncep.noaa.gov/products/analysis_monitoring/ensostuff/ensoyears.shtm.

The seven strongest EN events (7S_EN), 1957, 1965, 1972, 1982, 1986, 1991, 1997 were also considered. They were selected from the Hist_EN events, as being those with the largest values of the multivariate ENSO index (MEI). The MEI is calculated as the first unrotated principal component resulted from the combined empirical orthogonal analysis of six observed fields over the tropical Pacific: sea-level pressure, zonal and meridional components of the surface wind, SST, surface air temperature, and total cloudiness fraction of the sky (e.g. Wolter and Timlin, 2011). The MEI provides an integrated description of the oceanic and atmospheric conditions determining the ENSO activity, allowing a more refined comparison and ranking between different ENSO events than that provided by indices only based on oceanic conditions, such as the ONI.

Linear correlation and regression analysis were made to describe the climatological relationship between the

Table 1. Correlations between detrended values of the SAM and ONI for three different periods, 1957–2015, 1957–1985, and 1986–2015.

	FMA	MAM	AMJ	MJJ	JJA	JAS	ASO	SON	OND	NDJ	DJF	JFM
57–15	−0.167	−0.192	−0.005	0.128	0.199	0.170	0.061	−0.083	−0.292**	−0.316**	−0.216	−0.165
57–85	−0.303	−0.333*	0.012	0.304	0.202	0.083	0.009	0.023	−0.220	−0.287	−0.260	−0.252
85–15	−0.082	−0.095	−0.081	−0.004	0.203	0.263	0.134	−0.172	−0.411**	−0.546***	−0.313*	−0.302

Significant correlations are shown by the asterisks *** < 1%, ** < 5%, and * < 10%.

ENSO and SAM, including the assessment of the corresponding confidence levels. Also, composite maps were computed to analyse the associated hemispheric climate anomalies.

3. Results

3.1. EN–SAM relationship

Table 1 shows the linear correlation values between the ONI and SAM for different seasons and for three different periods, 1957–2015, 1957–1985, and 1986–2015. During JJA, JAS, and ASO (winter and early spring in the SH) correlations are positive but non-significant for any of the three periods. In SON, negative correlations are evident for the most recent and the full period, but they are not significant. On the other hand, negative correlations are large during OND, NDJ, and DJF for the three periods, being the largest and most significant those for the 1986–2015 period. From JFM to MAM, correlation values remain negative but almost all of them are non-significant. In agreement with previous studies (e.g. Silvestri and Vera, 2009), the table confirms that the SAM and ENSO are significantly anti-correlated mainly during late spring and early summer.

The SAM activity during EN events was analysed through the computation of boxplots of the corresponding SAM index values (Figure 1). In ASO, SON, and OND, i.e. is late winter and spring in the SH, the SAM exhibits considerable dispersion among the Hist_EN events ranging from negative to positive values. However, some progression towards more negative values as the year goes by is evident. In OND, the SAM index ranges between −3.11 and −0.40 in 50% of the Hist_EN events, while in the other 50% the index is between −0.40 and 1.48. In NDJ, which corresponds to late spring–early summer in the SH, around 60% of the SAM values for the Hist_EN events are negative with an extreme negative value associated with EN event of 1976/1977 of −3.72. Moreover, in DJF and JFM, summer in the SH, more than 70% of the events are associated with negative SAM values.

The SAM analysis for the 7S_EN events (Figure 1) shows that in ASO and SON the SAM is negative in around 57% of them. In SON, values extend between −2 and −0.82 in 50% of the 7S_EN events, while in the other 50% they are dispersed between −0.82 and 1.71. In OND, the tendency for more negative SAM values is evident, being in 50% of the 7S_EN events between −3.11 and −0.40. In NDJ and DJF, values are negative in six of the 7S_EN

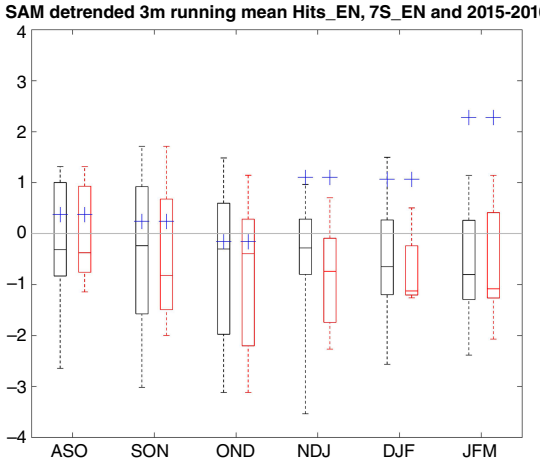

Figure 1. Boxplots of the detrended SAM values associated with the Hist_EN events (blue) and 7S_EN events (red) for ASO, SON, OND, NDJ, DJF, and JFM. Crosses indicate the SAM values for the seasons of 2015–2016. [Colour figure can be viewed at wileyonlinelibrary.com].

events with medians of −0.74 and −1.13 respectively. In JFM, values are negative in five of the 7S_EN events with a median of −0.9.

During 2015, SAM index values were moderately positive in ASO and SON while almost negligible in OND, being all these values within the range of those historically associated with both Hist_EN and 7S_EN events. However, in NDJ and DJF of 2015–2016, SAM remained positive with values at around 1, and it increased up to around 2.5 in JFM. These SAM magnitudes have never occurred neither in NDJ nor in JFM for any of the EN events considered. DJF SAM index attained values as high only in 1994–1995 (season considered within the Hist_EN events but not in 7S_EN events).

The SAM–ENSO relationship was further analysed for NDJ. A scatter diagram was computed between the SAM index and MEI over the April 1957–March 2015 period, and complemented with the linear regressions estimated between the two of them separately for the early period, 1957–1985, and for the late one considered, 1986–2015 (Figure 2). Between 1957 and 1985, a negative relationship is discernible between the SAM and MEI, but associated with large uncertainties and a non-significant linear regression coefficient of −0.42. On the other hand, during the most recent period, 1986–2015, the negative linear relationship between SAM and MEI is larger and significant (regression coefficient of −0.5) and the uncertainty band is narrower. An analysis of the *y*-intercept values shows that for the 1957–1985 period it is negative but

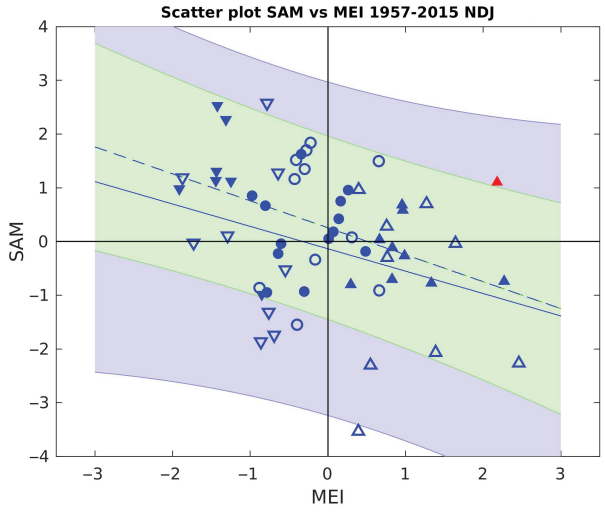

Figure 2. Scatter plot between detrended values of SAM and MEI for NDJ for the period 1957–2015. Triangles denote EN years, inversed triangles LN years, and dots represent neutral years. Open (solid) symbols correspond to the period 1957–1985 (1986–2015). Red triangle depicts EN 2015–2016. Lines represent linear regressions for the period (solid) 1957–1985 and (dashed) 1986–2015. Associated uncertainty bands are shadowed in blue (light green) for the period 1957–1985 (1986–2015). [Colour figure can be viewed at wileyonlinelibrary.com].

non-significant (−0.13), while for the 1986–2015 period it is positive and significant (0.25). During the 1957–1985 period, the values associated with EN 1976–1977 fall outside the uncertainty band characterizing the linear regression between SAM and MEI. It corresponds to the strongest negative SAM value and a positive but weak MEI. On the other hand, between 1986 and 2015 all the values for the period are within the corresponding uncertainty range excepting that associated with the EN15–16, confirming its outlier distinctive characteristic.

3.2. Circulation anomalies in the SH

A comparative analysis of the NDJ mean circulation anomalies observed in the SH in association with Hist_EN, 7S_EN, and EN15–16 was made. The composites of the 200-hPa geopotential-height anomalies for Hist_EN events (Figure 3a) exhibit a strong centre of positive anomalies over the Antarctica and a band of negative anomalies at middle latitudes, with evidences of a wavenumber 3–4 structure. The pattern resembles very much to that associated with the SAM negative phase. Also, an alternation of anomalies of positive and negative sign extended from the tropical portions of the central Pacific and western Indian Oceans to the Antarctica Peninsula and the South Atlantic is discernible too. The latter looks like the so-called Pacific-South America (PSA) patterns, which are considered the typical response of the circulation anomalies in the SH to ENSO (e.g. Mo, 2000). Vera *et al.* (2004) show that the changes induced by a negative SAM phase in the circulation anomalies in the SH during austral spring of EN years reinforce the PSA influence. At 30 hPa, a distinctive positive anomaly monopole is located over the Antarctica (Figure 3d), suggesting that the influence of the SAM negative phase is well extended at both the troposphere and stratosphere.

The circulation anomaly composites for the 7S_EN events also show evidences of a SAM negative phase combined with PSA-like patterns, but with larger anomalies and more evident zonal asymmetries at middle latitudes (Figure 3c). At 30 hPa, the positive circulation anomaly is also present, but being stronger for the 7S_EN events than for the Hist_EN ones. It is worth mentioning that, in both cases, despite composites are computed including many years before 1979, the overall structure observed is in agreement with previous works (e.g. Mo, 2000; Vera *et al.,* 2004).

The composite 200-hPa geopotential-height anomalies for EN15–16 event (Figure 3c) exhibit at tropical and subtropical latitudes essentially the same sign than those found for both, Hist_EN and 7S_EN events (Figures 3a, b). However, they are considerable different poleward. In the EN15–16 event, large negative anomalies are well discernible over the Antarctica that are typical of SAM positive phases. In addition, the negative centres located over central and eastern portions of the south Pacific middle latitudes and the positive centre extended to the west of the Antarctic Peninsula are shifted equatorward in the EN15–16 than in the other EN composites, in agreement with Fogt (2016). Moreover, the negative anomaly centre extended over the south central Atlantic in both Hist_EN and 7S_EN events (Figures 3a, b, respectively) is located poleward in the EN15–16 event (Figure 3c). At 30 hPa, a large and negative anomaly centre spans over the Antarctica and surrounding oceans in EN15–16 (Figure 3f). The latter is in agreement with the assessment made by CPC (2015) and Nash *et al.* (2016), which documented a stratospheric polar vortex particularly intense and persistent during the austral spring of 2015.

3.3. Impact on surface air temperature in the Antarctic Peninsula

Composites of NDJ surface air temperature anomalies for Hist_EN are weakly positive over part of the Antarctic continent and almost negligible over the Antarctic Peninsula (Figure 4a). They are somewhat larger and positive for 7S_EN events (Figure 4b) but they are large and negative in the EN15–16 event (Figure 4c). The analysis of Figure 3 shows that while both, Hist_EN and 7S_EN events, are associated with anticyclonic anomalies extended over the Antarctic continent and maximizing off the western Antarctica coast, negative circulation anomalies characterize the Antarctic region in the EN15–16 event. The latter are associated with stronger than normal subpolar westerlies, which promote large and negative temperature anomalies over most of the Antarctica continent, including the Antarctic Peninsula (Figure 4c).

Variations in the ENSO-related forcing over the Antarctic Peninsula can be at least partially associated with the ENSO–SAM relationship (e.g. Clem and Fogt, 2013). Clem *et al.* (2016) showed that in summer, Antarctic Peninsula temperature anomalies are not significantly

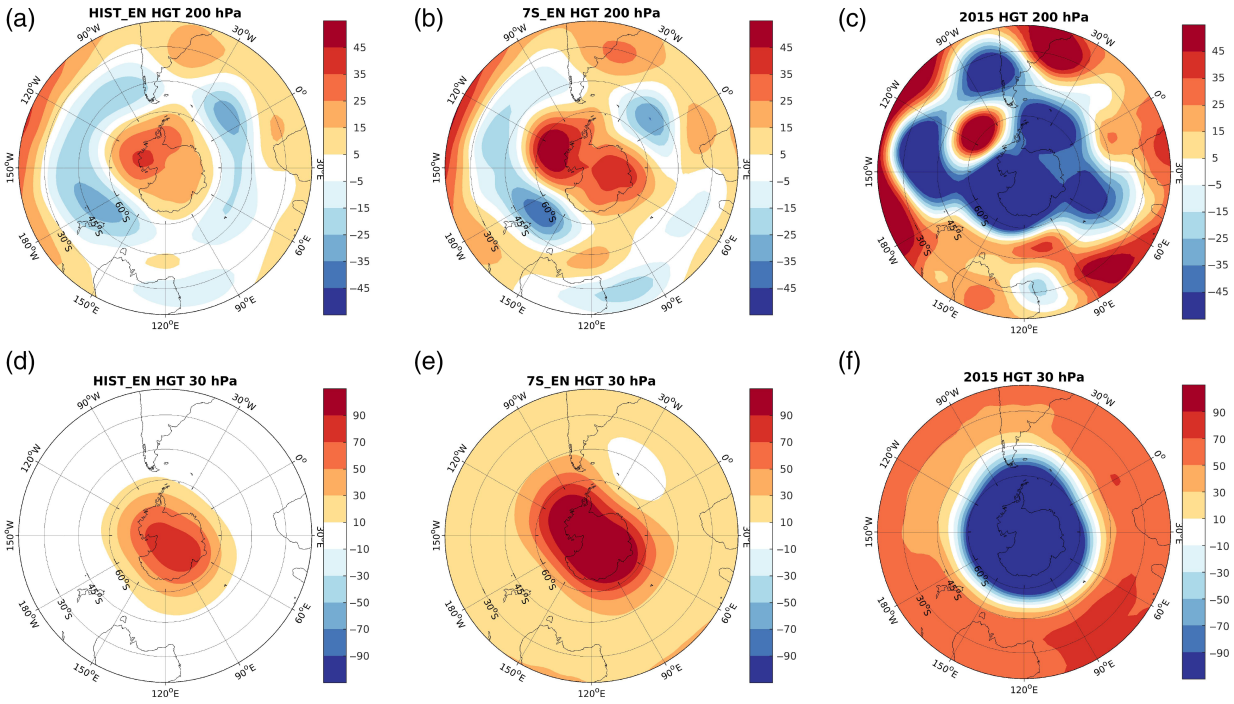

Figure 3. Composites of NDJ 200-hPa geopotential-height anomalies for (a) Hist_EN, (b) 7S_EN, and (c) EN 2015–2016. Composites of NDJ 30-hPa geopotential-height anomalies for (d) Hist_EN, (e) 7S_EN, and (f) EN 2015–2016. [Colour figure can be viewed at wileyonlinelibrary.com].

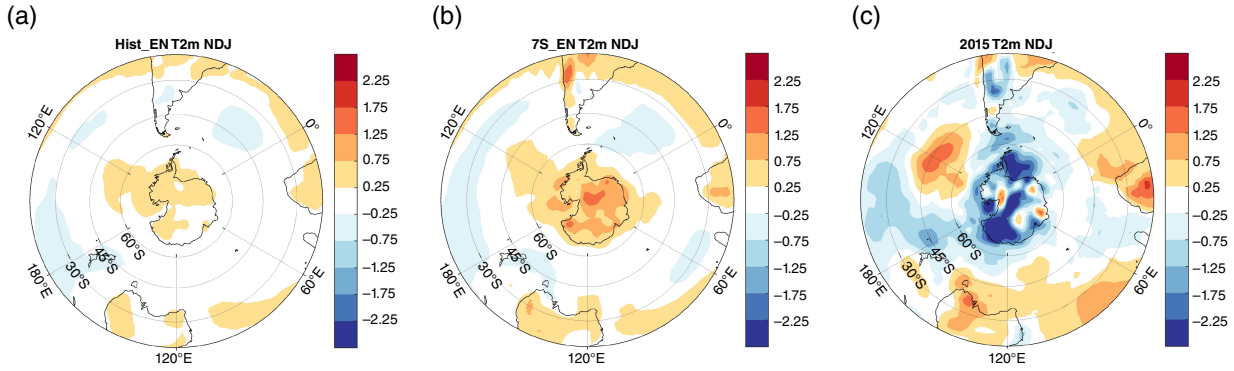

Figure 4. Composites of NDJ 2-m air temperature anomalies for (a) Hist_EN, (b) 7S_EN, and (c) EN 2015–2016. [Colour figure can be viewed at wileyonlinelibrary.com].

correlated with ENSO, after removing SAM influence. Instead, DJF temperature anomalies over the west side of the Antarctic Peninsula are significantly anticorrelated with SAM, after removing ENSO signal.

Surface air temperature anomalies in the Antarctic Peninsula were further analysed using data from the stations of Jubany, Esperanza, San Martin, and Marambio, which are available for slightly different periods (Table 2). Boxplots of the temperature anomaly values (Figure 5) show that during the EN15–16 event, the four stations exhibited colder than normal conditions in NDJ, DJF, and JFM. Moreover, negative anomalies were larger in magnitude for the stations located on the western portion of the Antarctic Peninsula (Jubany, San Martin) than those observed over the east of the peninsula (Esperanza and Marambio). These results agree with those obtained by Clem *et al.* (2016), confirming the important role of the SAM activity in determining the temperature anomalies in west Antarctic Peninsula. Figure 5a also shows that temperature anomalies at Jubany for EN15–16 event fall in the first quartile in NDJ and DJF. However, the negative ones observed for this particular EN event at San Martin in NDJ, DJF, and JFM never occurred during any of the Hist_EN events considered in the available period (Figure 5c).

Table 2. Location and surface pressure data availability of Antarctic stations analysed in this study.

Station	Latitude	Longitude	Data availability	Missing months
Jubany	62.2°S	58.6°W	1986–2016	1
Esperanza	63°24′S	56°59′W	1961–2016	55
San Martín	68°S	67°W	1977–2016	5
Marambio	64°15′S	56°39′W	1971–2016	6

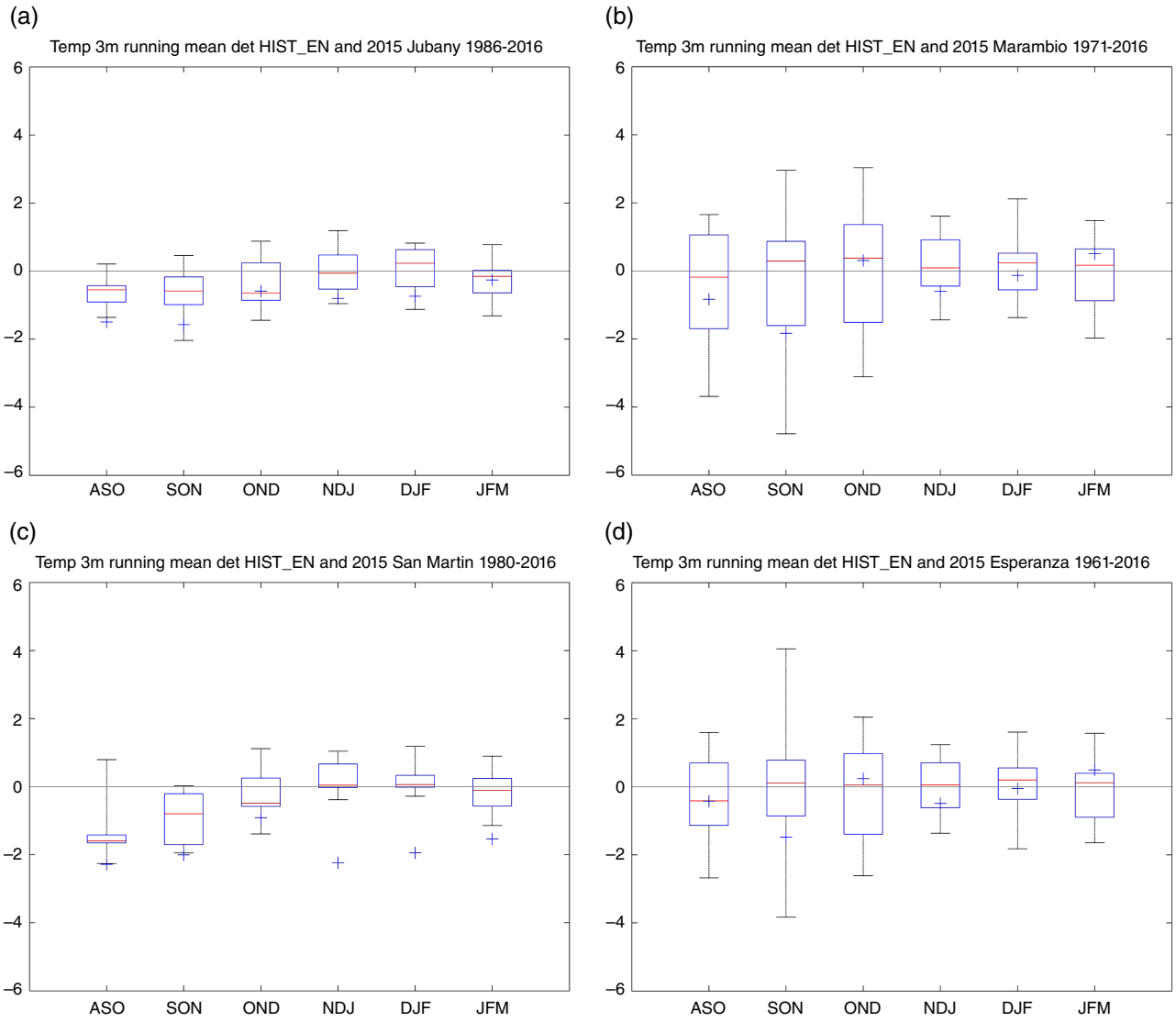

Figure 5. Boxplots of the detrended surface air temperature anomalies associated with the Hist_EN events for ASO, SON, OND, NDJ, DJF, and JFM, for the stations (a) Jubany, (b) Esperanza, (c) San Martín and (d) Marambio. Crosses indicate the values for the seasons of 2015–2016. [Colour figure can be viewed at wileyonlinelibrary.com].

3.4. Impact on precipitation anomalies in SESA

SESA is a region in which the influence, either separated or combined, of the ENSO and SAM on precipitation anomalies has been documented as significant, particularly during the austral seasons of spring and summer (e.g. Vera and Silvestri, 2009). Positive precipitation anomalies in SESA are correlated with EN events and SAM negative phases. Boxplots of precipitation anomalies in SESA (defined as the area between 56–64°W and 30–34°S) for the Hist_EN events show that most of the values are positive and in many cases large (Figure 6). This characteristic is also evident for the 7S_EN events, which are associated with precipitation anomalies especially larger in NDJ and DJF (Figure 6). However, precipitation anomalies in SESA for the EN15–16 are negligible in DJF and unusually negative in JFM, falling out of the range of values observed in any of the EN events considered. Considering the extraordinary positive values that SAM achieved in DJF and JFM for the EN15–16 event (Figure 1), it can be speculated that, besides the large intensity of the EN15–16, the SAM influence dominated onto SESA precipitation anomalies.

4. Concluding remarks

The study describes the main characteristics associated with the activity of the SAM during the EN15–16 event and its influence on climate anomalies in the SH, in comparison to what historically happened in previous EN events. In the period between December 1957 and March 2015, the relationship between ENSO and SAM is on average negative during the austral seasons of spring and early summer, and particularly significant in the more recent period (1986–2014). Moreover, the strongest EN events (7S_EN) are in general more frequently related with negative SAM phases during those two seasons.

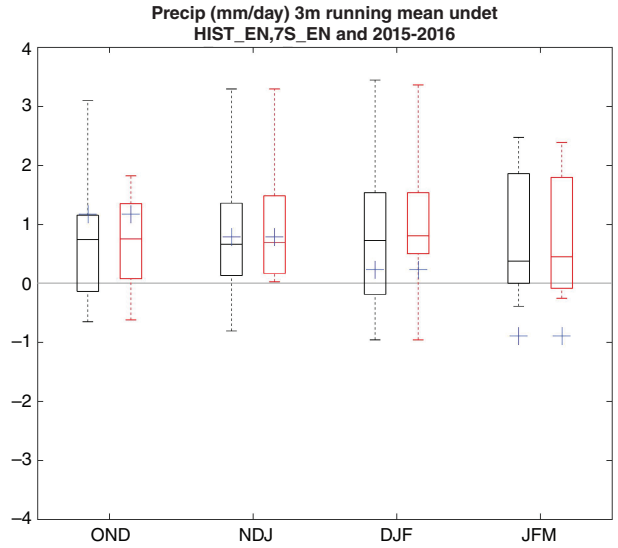

Figure 6. Same as Figure 1 but for precipitation anomalies in SESA (56–64°W and 30S–34°S). [Colour figure can be viewed at wileyonlinelibrary.com].

The EN15–16 was one of the three strongest events ever recorded. However, it was associated with unusually intense SAM positive phases, never recorded in spring and early summer during any of the 7S_EN events.

The analysis of the linear relationship observed between ENSO and SAM in NDJ shows that between 1986 and 2015, it was significantly negative and associated with a narrow uncertainty band. However, the combined condition of ENSO and SAM in the EN15–16 event (both associated with large positive phases) is an outlier. Moreover, an increase of the *y*-intercept magnitude was observed from the 1957–1985 period to the most recent one, in which it became positive. The latter allows to speculate that the behaviour detected during the EN15–16 (i.e. EN event associated with positive SAM phase) although it is still an outlier, it could be less rare if the ENSO–SAM linear relationship varies in the future in a similar manner.

The composites of the circulation anomalies in the SH for the Hist_EN and 7S_EN events resemble the typical combination of a PSA-like patterns superimposed with that associated with a SAM negative phase, being the latter observed not only at the troposphere but also in the stratosphere. On the other hand, the circulation anomalies for the EN15–16 show clear evidences of a pattern resembling the positive SAM phase, which altered the development of the extratropical circulation anomalies associated with the ENSO-induced PSA pattern.

The hemispheric circulation anomalies in the EN15–16 promoted unusually negative surface air temperature over the Antarctic continent and, in particular, over the Antarctic Peninsula. The analysis of the surface air temperature anomalies at four stations located in the Antarctic Peninsula shows that in spring and early summer, they were negative for the EN15–16. Moreover, they were particularly extreme, as compared to those observed in the past EN events, for the stations located over the western coast of the Peninsula.

The circulation anomalies in the EN15–16 strongly influenced by the large positive SAM phase also altered the typical EN influence on precipitation anomalies in SESA. While during spring and summer anomalies related with EN events are in general positive, and particularly large with the strongest EN events, during the EN15–16 they were unusually negative with a magnitude never recorded in JFM for any EN event occurred between 1957 and 2014.

The results of this analysis have important implications for the climate prediction of ENSO impacts in the SH. Further research exploring the causes of the SAM behaviour during 2015 and 2016 and an assessment of their predictability levels are needed.

Acknowledgements

The research was supported by Consejo Nacional de Investigaciones Científicas y Técnicas (CONICET) PIP 112-20120100626CO, UBACyT 20020130100489BA, PIDDEF 2014/2017 Nro 15, Belmont Forum/ANR-15-JCL/-0002-01 CLIMAX. M.O. was supported by a postdoctoral grant from CONICET, Argentina.

References

Arblaster JM, Meehl GA. 2006. Contributions of external forcings to southern annular mode trends. *J. Clim.* **19**(12): 2896–2905.

Arblaster JM, Meehl GA, Karoly DJ. 2011. Future climate change in the southern hemisphere: competing effects of ozone and greenhouse gases. *Geophys. Res. Lett.* **38**(2): L02701.

Baldwin MP, Dunkerton TJ. 2001. Stratospheric harbingers of anomalous weather regimes. *Science* **294**(5542): 581–584.

Clem KR, Fogt RL. 2013. Varying roles of ENSO and SAM on the Antarctic Peninsula climate in austral spring. *J. Geophys. Res. Atmos.* **118**(20): 11481–11492.

Clem KR, Renwick JA, McGregor J, Fogt RL. 2016. The relative influence of ENSO and SAM on Antarctic Peninsula climate. *J. Geophys. Res. Atmos.* **121**(16): 9324–9341. https://doi.org/10.1002/2016JD025305.

Climate Prediction Center (CPC). 2015. Climate diagnostic bulletin. Near real-time ocean/atmosphere monitoring, assessments and prediction. Climate Prediction Center. http://www.cpc.ncep.noaa.gov/products/CDB/CDB_Archive_pdf/pdf_CDB_archive.shtml (accessed 11 January 2018).

Fogt RL. 2016. El Niño and Antarctica [in "state of the climate in 2015"]. *Bull. Am. Meteorol. Soc.* **97**(8): S162.

Fogt RL, Bromwich DH. 2006. Decadal variability of the enso teleconnection to the high-latitude south pacific governed by coupling with the southern annular mode. *J. Clim.* **19**(6): 979–997.

Fogt RL, Bromwich DH, Hines KM. 2011. Understanding the SAM influence on the south pacific ENSO teleconnection. *Clim. Dyn.* **36**(7): 1555–1576.

Kalnay E, Kanamitsu M, Kistler R, Collins W, Deaven D, Gandin L, Iredell M, Saha S, White G, Woollen J, Zhu Y, Leetmaa A, Reynolds R, Chelliah M, Ebisuzaki W, Higgins W, Janowiak J, Mo KC, Ropelewski C, Wang J, Jenne R, Joseph D. 1996. The NCEP/NCAR 40-year reanalysis project. *Bull. Am. Meteorol. Soc.* **77**(3): 437–471.

Kidson JW. 1988. Interannual variations in the southern hemisphere circulation. *J. Clim.* **1**(12): 1177–1198.

Kidson JW. 1999. Principal modes of southern hemisphere low-frequency variability obtained from NCEP-NCAR reanalyses. *J. Clim.* **12**(9): 2808–2830.

Marshall GJ. 2003. Trends in the southern annular mode from observations and reanalyses. *J. Clim.* **16**(24): 4134–4143.

Mo KC. 2000. Relationships between low-frequency variability in the southern hemisphere and sea surface temperature anomalies. *J. Clim.* **13**(20): 3599–3610.

Nash ER, Strahan SE, Kramarova N, Long CS, Pitts MC, Newman PA, Johnson B, Santee ML, Petropavlovskikh I, Braathen GO. 2016. Antarctic ozone hole [in "state of the climate in 2015"]. *Bull. Am. Meteorol. Soc.* **97**(8): S166–S172.

Silvestri G, Vera C. 2009. Nonstationary impacts of the southern annular mode on southern hemisphere climate. *J. Clim.* **22**(22): 6142–6148.

Vera C, Silvestri G. 2009. Precipitation interannual variability in South America from the WCRP-CMIP3 multi-model dataset. *Clim. Dyn.* **32**(7): 1003–1014.

Vera C, Silvestri G, Barros V, Carril A. 2004. Differences in El Niño response over the southern hemisphere. *J. Clim.* **17**(9): 1741–1753.

Wolter K, Timlin MS. 2011. El Niño/southern oscillation behaviour since 1871 as diagnosed in an extended multivariate enso index (MEI.ext). *Int. J. Climatol.* **31**(7): 1074–1087.

